ISSN 1000-9825, CODEN RUXUEW
Journal of Software, Vol.20, No.5, May 2009, pp.1106−1115
doi: 10.3724/SP.J.1001.2009.03547

E-mail: jos@iscas.ac.cn
http://www.jos.org.cn
Tel/Fax: +86-10-62562563

能量传导模型及在医学图像分割中的应用*

段侪杰[1], 马竟锋[2], 张艺宝[1], 侯 凯[3], 包尚联[1,3+]

[1](北京大学 重离子物理研究所 医学物理和工程北京市重点实验室,北京 100871)

[2](浙江大学 计算机科学学院,浙江 杭州 310027)

[3](北京海思威科技有限公司,北京 100080)

Energy Conduction Model and Its Application in Medical Image Segmentation

DUAN Chai-Jie[1], MA Jing-Feng[2], ZHANG Yi-Bao[1], HOU Kai[3], BAO Shang-Lian[1,3+]

[1](Beijing Key Lab of Medical Physics and Engineering, Institute of Heavy Ion Physics, Peking University, Beijing 100871, China)

[2](College of Computer Science, Zhejiang University, Hangzhou 310027, China)

[3](Beijing Healthware Science & Technology Inc. Lim., Beijing 100080, China)

+ Corresponding author: E-mail: bao@pku.edu.cn

Duan CJ, Ma JF, Zhang YB, Hou K, Bao SL. Energy conduction model and its application in medical image segmentation. *Journal of Software*, 2009,20(5):1106−1115. http://www.jos.org.cn/1000-9825/3547.htm

Abstract: This paper proposes an energy conduction model (ECM) based on the level set framework, which takes advantage of the heat conduction equation to construct the image energy. After comparing the image intensity distribution with the spatial distribution of the temperature field, an energy conduction function is defined, which well simulates the process of heat conducting. The advantage of the ECM is that it captures the global feature of an image and takes the local intensity information into account. Thus, ECM is able to accurately segment medical images with inhomogeneity and noise, as well as for the medical images with multi-targets. Synthetic and real medical images are tested with ECM, which shows its robustness and efficiency.

Key words: energy conduction model; level set framework; C-V model; multi-targets segmentation; medical image segmentation

摘 要: 提出了一种基于水平集框架的能量传导模型ECM(energy conduction model)用于对医学图像进行分割.该模型通过对图像中的灰度分布和空间中的温度场分布进行对比,有效定义了图像能量和图像能量的传导方程,并通过模拟热量传递的过程对方程进行求解.ECM 模型的优点在于,它在描述图像灰度分布的全局特征的同时,有效地捕捉到图像局部区域的灰度对比度变化,因此它能够对灰度分布不均匀和含有噪声的图像进行精确分割.基于水平集函数本身的拓扑可变性,该方法还能够实现同一图像中的多目标分割.使用该方法对模拟和真实的医学图像进行

* Supported by the National Natural Science Foundation of China under Grant Nos.10527003, 60672104 (国家自然科学基金); the National Basic Research Program of China under Grant No.2006CB705705 (国家重点基础研究发展计划(973)); the Joint Research Subject of Beijing Education Committee of China under Grant No.JD100010607 (北京市共建项目); the Beijing Municipal Natural Science Foundation of China under Grant No.3073019 (北京市自然科学基金); the Upgrading Subject of Instrument in Science and Technological Ministry of China under Grant No.2006JG1000 (科技部仪器升级改造项目)

Received 2008-08-27; Accepted 2008-12-15

了分割实验,实验结果表明了该方法的有效性和可靠性.
关键词: 能量传导模型;水平集;C-V 模型;多目标分割;医学图像分割
中图法分类号: TP391 **文献标识码:** A

1 Introduction

Level set framework (LSF) is a geometric deformable model which was first introduced in 1988 by Osher and Sethian[1]. It was widely developed and applied in medical image processing, especially in image segmentation process. Usually, the boundaries of segmented regions in an image are derived by evolving the level set function and are represented by the zero level set curves. Since the level set function is of topological flexibility, it is suitable for multiple target segmentation.

An important part of LSF is the curve evolution theory and its mathematical implementation capability. In the case of segmentation, a level set function evolves according to an image force or energy. Previous works have constructed this force or energy with edge-based information, which requires acquiring the image edge in advance[2]. Also, other works use the region-based information that could segment image without edges[3−8]. Vese and Chan proposed region-based energy for multiphase segmentation (C-V model), which includes two cases: piecewise smooth case and piecewise constant case[3,4].

1.1 Piecewise constant case

The piecewise constant model is given by:

$$E_n(c,\phi)=\sum_{1\le I\le n=2^m}\int_\Omega (u_0-c_I)^2\chi_I \mathrm{d}x\mathrm{d}y+\sum_{1\le i\le m}\nu\int_\Omega |\nabla H(\phi_i)|\mathrm{d}x\mathrm{d}y \tag{1}$$

Here, E_n is an image energy function which includes m level set functions. The m level set functions segment an image into at the most n=2^m regions. $\Omega\subset\Re^2$ is an opened and bounded image domain. u_0:$\Omega\subset\Re$ is a given bounded image function. c_I is the mean intensity in region I. $H(\phi)$ is the Heaviside function, whose value is 1 when ϕ>0 and 0 when ϕ≤0. χ_I is the characteristic function implemented by the “vector Heaviside function” $\vec{H}(\phi)$. Here, $\vec{H}(\phi)=(H(\phi_1),...,\ H(\phi_m))$ is composed of 0 and 1. ν is a constant value. Since there is only one global feature in a region in the piecewise constant model, it cannot deal with the inhomogeneous problem.

1.2 Piecewise smooth case

The piecewise smooth model inherits the model proposed by Mumford and Shah (M-S model)[6] and applies the level set framework to search the optimal solution. By using smooth functions to approximate image function, it segments images into piecewise smooth regions. We note that another group did similar work independently and simultaneously[7,8]. Their work and C-V model are essentially the same. The differences lie on the algorithmic implementations and extensions.

The piecewise smooth model is given by

$$F_n(u,\phi)=\sum_{1\le I\le n=2^m}\int_\Omega (u_0-u)^2\chi_I \mathrm{d}x\mathrm{d}y+\sum_{1\le I\le n=2^m}\mu\int_\Omega |\nabla u|^2\chi_I \mathrm{d}x\mathrm{d}y+\sum_{1\le i\le m}\nu\int_\Omega |\nabla H(\phi_i)|\mathrm{d}x\mathrm{d}y \tag{2}$$

In this formula, the constant mean intensity value c_I is replaced by the piecewise smooth function u. The item $|\nabla u|$ guarantees u varying smoothly. μ is a constant value. All other parameters are of the same meaning as they are in Eq.(1).

Unlike the piecewise constant model, the piecewise smooth model segments images with intensity inhomogeneous correctly. However, for multi-target segmentation, the piecewise smooth model leads to problematic results. It may have more than one major intensity levels in one region. Thus, it relies more on the initial condition and is more sensitive to the control parameters.

The C-V model first used one level set function for two phase segmentations[3]. Then it was generalized to multiphase segmentation, which uses more than one level set functions to segment the image into more than two regions[4]. Theoretically, it is able to segment up to 2^n regions with only n level set functions. The multiphase level set scheme can represent triple junctions and complex topologies without producing “vacuum” and “overlap”. Other groups used the hierarchical method to solve the multiphase problem[7−13]. Compared with the hierarchical method, the multiphase level set method gives more accurate and detailed results[14].

Considering the constraints of C-V model, we introduce an energy conduction function combined with the multiphase level set framework which is energy conduction model (ECM). The ECM is able to capture major characteristic of each region as well as local intensity features. Therefore, it inherits the advantages of both piecewise constant model and piecewise smooth model while eliminating their defects. Although some medical image modalities such as MRI tend to have problems such as inhomogeneity and heavy noise, the ECM can give correct results for segmentation, which is effective even with a general initial condition of level set functions for most cases.

2 Energy Conductive Model

2.1 Assumption

The goal of our work is to solve the problems met by the C-V model, and find a way to segment inhomogeneous medical image with multi-targets in an image. The heat conduction theory is used. This model first assumes there are n regions in an image with each region having an identical temperature. The spatial temperature distribution function of each region is represented by $u_n(\bar{x})$. c_n is the major characteristic temperature of region n. Then, we assume that each pixel $I(\bar{x})$ in the image is a heat source with constant temperature equal to its intensity value, and contributes to the spatial temperature distribution function. Each heat source releases or absorbs energy if its temperature is higher or lower than the spatial temperature at the same position. After segmentation, the final steady state is reached in which the total energy transmission is minimized. The boundaries of segmentation results represent isolating layer, which prevent energy from conducting among separated regions. If n=2, this procedure is like closing the cold storage door in order to save energy.

2.2 Conducting energy

To meet the goal mentioned above, we introduced an image energy term called conducting energy E^{CE}. The conducting energy measures the quantity of heat transmission among the space.

$$E_{\bar{x}}^{CE}(L,c_1,c_2,u_1,u_2)=\lambda_1\int_{inside(L)}A(\bar{x}-\bar{y})((I(\bar{y})-c_1)-u_1(\bar{x}))^2\mathrm{d}\bar{y}+\lambda_2\int_{ouside(L)}A(\bar{x}-\bar{y})((I(\bar{y})-c_2)-u_2(\bar{x}))^2\mathrm{d}\bar{y} \tag{3}$$

Let L be the zero level set boundary. $\bar{x},\bar{y}$ are coordinate in denoting the position of each point. Eq.(3) is the quantity of energy transmitted at point $\bar{x}$, where λ_1 and λ_2 are positive constant values. c_i is the mean value of I in region i. $A(\bar{x}-\bar{y})$ is a weight parameter. Considering the possible noise, this parameter takes the points nearby into account and weigh them according to their distance to the central point $\bar{x}$. We choose $A(\bar{x}-\bar{y})$ as follows:

$$A(\bar{x}-\bar{y})=\frac{1}{|\bar{y}-\bar{x}|+\varepsilon} \tag{4}$$

ε is a small positive value, so that the denominator will never be equal to zero. The overall energy transmitted is the integral of energy transmission at every point.

$$E^{CE}(L,c_1,c_2,u_1,u_2)=\int_{\Omega}E_{\bar{x}}^{CE}(L,c_1,c_2,u_1,u_2)\mathrm{d}\bar{x} \tag{5}$$

Here, we redefine the temperature of heat sources according to the main characteristic temperature c_i in each region. Thus, in region i, the temperature of heat source at position $\bar{x}$ is $I(\bar{x})-c_i$. This transformation makes it possible to control the number of major temperature and ensure that there exists one and only one major temperature in one region. For example, if one level set function is used, then the image is divided into two regions while only one major temperature inside and one outside the zero level set curves respectively.

As in C-V model, we use Lipschitz function ϕ as the level set function and use Heaviside function $H(\phi)$ to describe different regions. Therefore, the conductive energy in Eq.(5) is written as:

$$\begin{aligned} E^{CE}(\phi,c_1,c_2,u_1,u_2) = {} & \lambda_1\int\left(\int A(\bar{x}-\bar{y})((I(\bar{y})-c_1)-u_1(\bar{x}))^2 \mathrm{d}\bar{y}\right)H(\phi(\bar{x}))\mathrm{d}\bar{x} + \\ & \lambda_2\int\left(\int A(\bar{x}-\bar{y})((I(\bar{y})-c_2)-u_2(\bar{x}))^2 \mathrm{d}\bar{y}\right)(1-H(\phi(\bar{x})))\mathrm{d}\bar{x} \end{aligned} \tag{6}$$

Besides the energy generated from the image information, we still need another term to control the geometrical property. In most applications, the length of zero level set contour is used, which is given by

$$L(\phi)=\int_{\Omega}|\nabla H(\phi(\bar{x}))|\mathrm{d}\bar{x} \tag{7}$$

Combining Eqs.(6) and (7), we get the final energy function

$$F(\phi,c_1,c_2,u_1,u_2)=E^{CE}(\phi,c_1,c_2,u_1,u_2)+\nu L(\phi) \tag{8}$$

2.3 Heat conduction and gradient decent flow

The energy function is minimized by use of gradient decent flow. It alternates between iterating the temperature distribution function and the Lipschitz function ϕ.

The temperature distribution function evolves according to the heat conduction law. And we write it as:

$$H(\phi)\frac{\partial u_1}{\partial t}=\mu_1 H(\phi)(I-c_1-u_1)+\mu_2\nabla\bullet(H(\phi)g(|\nabla u_1|)\nabla u_1) \tag{9}$$

$$(1-H(\phi))\frac{\partial u_2}{\partial t}=\mu_1(1-H(\phi))(I-c_2-u_2)+\mu_2\nabla\bullet((1-H(\phi))g(|\nabla u_2|)\nabla u_2) \tag{10}$$

In Eqs.(9) and (10), we assume that the heat conduction is an anisotropic procedure. In the steady state, the temperature distribution function should be as smooth as possible. In our model, we use an anisotropic conduction coefficient $g(|\nabla u|)$. Previous work uses similar anisotropic coefficient for edge detection[15] and preprocessing for image segmentation[16]. Inversely, we use anisotropic diffusion to diminish the variation within one region. We simply set $g(|\nabla u|)$ to be

$$g(|\nabla u|)={}^{|\nabla u|}\!\big/_{K} \tag{11}$$

K is a positive constant.

Another issue remained is how to extend the temperature distribution function out of its definition domain. In our model, the distance function is used. If we let the temperature distribution functions “diffuse” from region boundaries along the normal direction of the distance function inwards or outwards monotonically, then the temperature distribution functions are well extended. We again use an anisotropic diffusion parameter $c(\phi)$ to control the “diffusion”. This procedure is described in Eq.(12):

$$\frac{\partial u_e}{\partial t}=\nabla\bullet(c(\phi)\nabla u_e) \tag{12}$$

u_e is the extension of temperature distribution function u_i. We denote the definition domain of u_i as “inside” and the definition domain of u_e as “outside”. The temperature distribution extends from inside through outside monotonously. Again, we rewrite Eq.(12) as follows:

$$u_{e,i,j}^{n+1}=\frac{c_1(\phi)u_{e,i+1,j}^n+c_2(\phi)u_{e,i-1,j}^n+c_3(\phi)u_{e,i,j+1}^n+c_4(\phi)u_{e,i,j-1}^n}{C(\phi)} \tag{13}$$

where, $c(\phi)=c_1(\phi)+c_2(\phi)+c_3(\phi)+c_4(\phi)$, and $c_i(\phi)$ (i=1,2,3,4) has different expressions at different conditions. If ϕ>0 is the “inside”, then

$$\begin{aligned}
c_1(\phi_{i,j}) &= \max((\phi_{i+1,j}-\phi_{i,j}),0) \text{ in } \{\phi(x,y)\le 0\}\\
c_2(\phi_{i,j}) &= -\min((\phi_{i,j}-\phi_{i-1,j}),0) \text{ in } \{\phi(x,y)\le 0\}\\
c_3(\phi_{i,j}) &= \max((\phi_{i,j}-\phi_{i,j+1}),0) \text{ in } \{\phi(x,y)\le 0\}\\
c_4(\phi_{i,j}) &= -\min((\phi_{i,j}-\phi_{i,j-1}),0) \text{ in } \{\phi(x,y)\le 0\}
\end{aligned} \tag{14}$$

If $\phi\le 0$ is the “inside”, then

$$\begin{aligned}
c_1(\phi_{i,j}) &= -\min((\phi_{i+1,j}-\phi_{i,j}),0) \text{ in } \{\phi(x,y)\ge 0\}\\
c_2(\phi_{i,j}) &= \max((\phi_{i,j}-\phi_{i-1,j}),0) \text{ in } \{\phi(x,y)\ge 0\}\\
c_3(\phi_{i,j}) &= -\min((\phi_{i,j}-\phi_{i,j+1}),0) \text{ in } \{\phi(x,y)\ge 0\}\\
c_4(\phi_{i,j}) &= \max((\phi_{i,j}-\phi_{i,j-1}),0) \text{ in } \{\phi(x,y)\ge 0\}
\end{aligned} \tag{15}$$

Practically, $c_i(\phi)$ can be simplified to be 1 if $c_i>0$ and a small value δ if $c_i=0$.

After the establishment of the temperature distribution function, we turn to process the level set function. Since only the Lipschitz function ϕ is a variable in this step, we minimize the energy function with respect to ϕ. The gradient decent flow is derived:

$$\frac{\partial\phi}{\partial t}=-\delta(\phi)\left[\lambda_1\int A(\bar{x}-\bar{y})((I(\bar{y})-c_1)-u_1(\bar{x}))^2\mathrm{d}\bar{y}-\lambda_2\int A(\bar{x}-\bar{y})((I(\bar{y})-c_2)-u_2(\bar{x}))^2\mathrm{d}\bar{y}-\nu\nabla\bullet\left(\frac{\nabla\phi}{|\nabla\phi|}\right)\right] \tag{16}$$

Besides evolving the level set function, the method that we used to set narrowband and to reinitialize distance function can be found in our previous work[17] and the details of numerical implementation can be found in Refs.[4,18–20].

2.4 Flowchart of the segmentation procedure

The flowchart of the overall segmentation procedure is depicted in Fig.1. Firstly, the level set function is initialized and the image is divided into different regions by the zero level set curve. The initialized zero level set curve is expected not to be far from the final destination if the prior knowledge is applicable to reduce the calculation complexity and improve segmentation precision. To construct the image energy, in the second and third step, the temperature distribution function of each region i is initialized by setting $u_i=0$ and the major characteristic temperature in each region is given by the mean value of all heat sources I in the same region. Before evolving the level set function, the temperature distribution functions u_i are obtained by solving Eqs.(9) and (10) iteratively. A predefined maximum iterating number is used to stop this procedure and the approximate solutions are obtained. In the fifth step, the temperature distribution functions are introduced to the conducting energy in Eq.(6) which is minimized by evolving the level set function. As in Eq.(16), an artificial time t is used. If less than one tenth of the points on the zero level set curve move within one time step which is the stop criterion for the level set function evolution, then the level set function stop evolving. The procedure turns back to the second step for a new round calculation based on the segmentation result from the last iteration. The whole procedure stops when the level set evolution meets its stop criterion in the first time step.

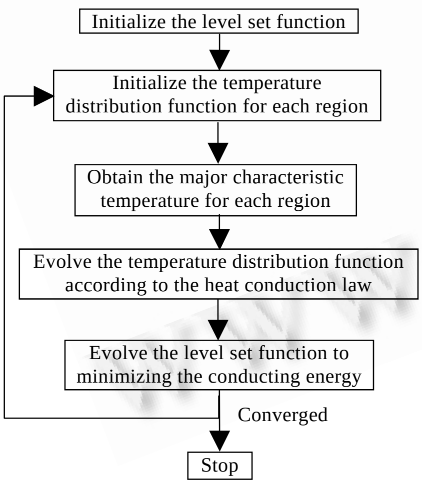

Fig.1 Flowchart of energy conduction model for medical image segmentation

3 Experiments and Results

We tested ECM with a variety of images and compared the results with those got from C-V model. All images used are gray-scale images in the range of 0 to 255.

The first tested image is a synthetic black ball image shown in Fig.2(a), which has inhomogeneous intensity. The results obtained from different algorithms are shown in Fig.2. Because the intensity of upper part of the ball is close to the background, the piecewise constant model gave incorrect result while the piecewise smooth model and the ECM gave better segmentation.

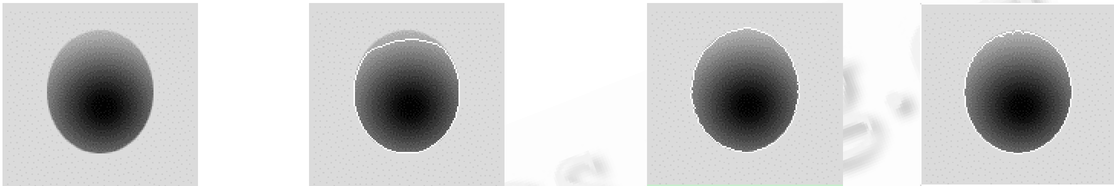

(a) Original image (b) Result of piecewise constant model (c) Result of piecewise smooth model (d) Result of ECM

Fig.2 Synthetic image

In Fig.3, an image containing three intensity levels is presented. We assume that the dark rounded region is a cell nucleus and the bright rounded region is impurity in a microscope cell image whose intensity values are lower and higher than the background respectively. The piecewise smooth model segmented both the nucleus and the impurity into one region while our ECM only picked the nucleus out. That is the problem of piecewise smooth model. It is regardless of the main intensity level and tends to over-segment images.

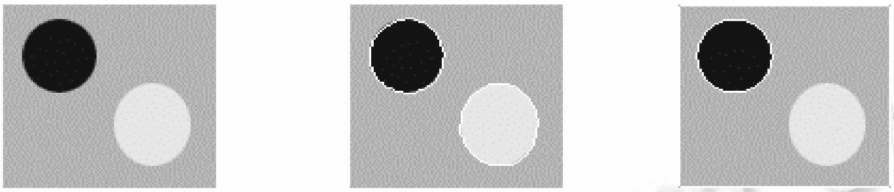

(a) Original image (b) Result of piecewise smooth model (c) Result of ECM

Fig.3 Synthetic image

The third test was for a more complicated synthetic image shown in Fig.4(a), which was segmented using two lever set functions. The image was segmented by use of the multiphase level set scheme proposed in C-V model, which could be imagined as a microscope cell image. The image has many cells and each cell contains nucleus and cytoplasm. The one at the top left has constant intensity values in nucleus and cytoplasm respectively. The intensity value of the nucleus at the bottom is varying gradually from the foreground to background and the same condition happens to the cytoplasm of the cell at the right side. Figure 4(b) and (c) are the segmented results by piecewise constant model and ECM. In Fig.4(b), the nucleus of the cell at the bottom was not segmented completely. But ECM gave the much better result (Fig.4(c)). Figure 4(d) and (e) give an example of the level set function evolution. Figure 4(d) depicts the initial zero level set curves and Fig.4(e) is the curve after several iterations. In this case, with the same initial condition, the piecewise smooth model gave meaningless result. It did not give a integral nucleus and cytoplasm but discrete smooth patches.

To test the robustness of our model, we applied white Gaussian noise to the image in Fig.4 and showed it in Fig.5(a). The segmented results showed that ECM is better than other models.

Figure 6 shows the intensity distribution of pixels on a horizontal scan line on the noisy image in Fig.5. The dash line in each diagram depicts the pixel's value on the noisy image. The solid line in Fig.6(a) labels each pixel by using the combination of temperature distribution function u_i and the major temperature level c_i. And the solid line in Fig.6(b) labels each pixel by the major temperature value of the region to which it belongs. Our model eliminated the influences from the noises and inhomogeneity.

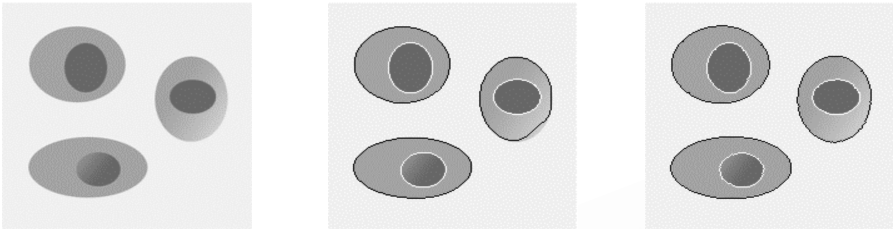

(a) Original image (b) Result of piecewise constant model (c) Result of ECM

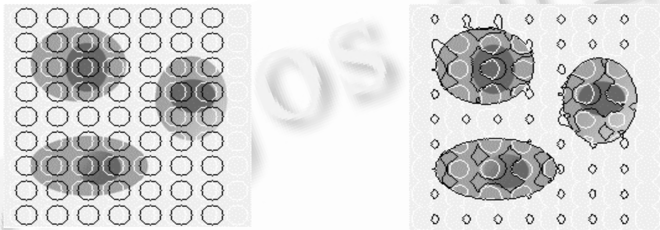

(d) Initialization of zero level set curve (e) Zero level set curve after several iteration

Fig.4 Synthetic microscope cell image

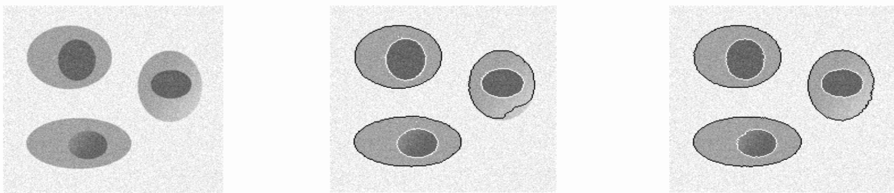

(a) Original image (b) Result of piecewise constant model (c) Result of ECM

Fig.5 Synthetic microscope cell images with white Gaussian noise

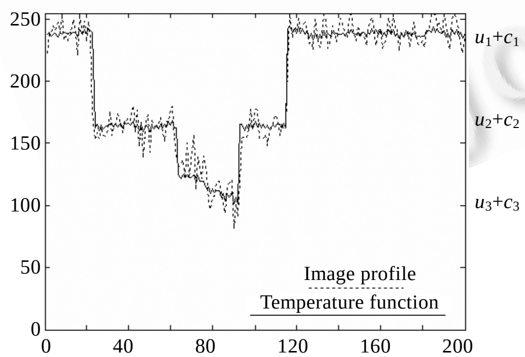

(a) Image profile and the combination of temperature distribution function and major temperature

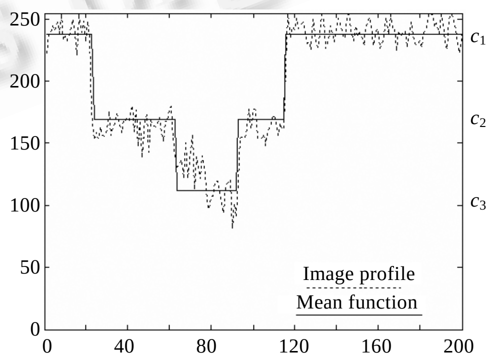

(b) Image profile and major temperature

Fig.6 Energy conduction model

Figure 7 uses a real microscope cell image. It used two level set functions to segment cells into nuclei and cytoplasm simultaneously. In Fig.8, a T1-weighted MR image of brain is segmented into four regions. Each region is depicted in Fig.8(d)~(g) respectively. The white matter, gray matter and cerebrospinal fluid are extracted. Figure 9 is a MRI image of stomach. We segmented the image into two regions in Fig.9(b) and four regions in Fig.9(c). In both cases, the stomach is distinctly picked out.

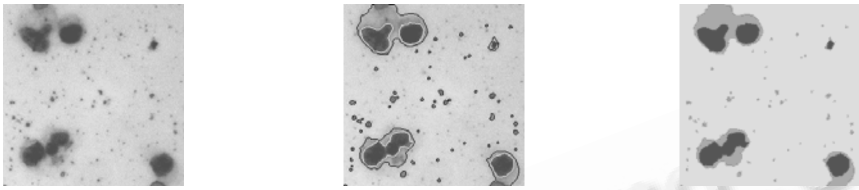

(a) Original image (b) Result of ECM expressed by zero level set curves (c) Result of ECM expressed by characteristic temperature value of each region

Fig.7 Real microscope cell segmentation results

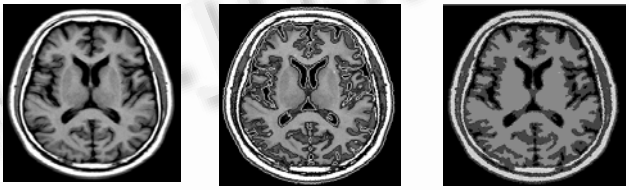

(a) (b) (c)

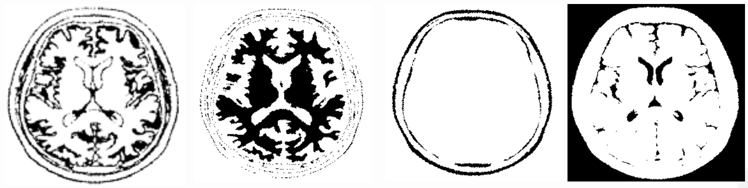

(d) (e) (f) (g)

(a) Original image
(b)~(c) Segmenting results expressed using zero level set curves and mean intensity
(d)~(g) Display four regions respectively with foreground in black and background in white

Fig.8 Segmenting MRI brain image using ECM

(a) Original image (b) ECM with one level set function (c) ECM with two level set functions

Fig.9 An MRI image of stomach

4 Discussion

In this paper, we proposed an energy conduction model for medical image segmentation. Compared with the C-V model, our model is more specialized for medical image segmentation. In C-V model, the piecewise constant model can not segment inhomogeneous region correctly as showed in Fig.2. The piecewise smooth model segments images into, as its name indicates, piecewise smooth patches and tends to include more than one major intensity level in one region. In our tests, the piecewise smooth model gave correct results only when the initial condition of level set function was designed specifically for each individual case. However, the ECM model is not sensitive to the initial condition. Actually all the tested examples shown above used the same initial condition as in Fig.3(d). Thus, the C-V model is not suitable for medical image segmentation in most conditions, but the ECM performs well.

The ECM contains complex parameters. Though it gave better results than C-V model in most cases, tuning the parameters of our model still affected the final results. Searching for a set of optimized parameters could give better segmentation results, but it is a time-consuming and tough job. However, in most of the cases, a set of optimized parameters are often available for segmenting images of the same modality.

5 Conclusion

In this paper, we propose an energy conduction model based on the multiphase level set scheme. The proposed model takes advantage of the heat conduction law. It describes the image energy as a spatial temperature distribution function and assumes each pixel as a heat source. We get the segmentation results by minimizing the quantity of conducting energy. We have applied this model to segment synthetic and real medical images. It is not sensitive to noise and can be used to segment images with low signal to noise ratio. Tests showed that an image was segmented into different regions with the intensity distribution of each region relatively similar at local and inhomogeneous throughout the whole image. ECM has the advantages of C-V model, and modifies its defects in medical image segmentation. The future work will focus on improving the efficiency of the ECM.

References:

[1] Osher S, Sethian J. Fronts propagating with curvature dependent speed: algorithms based on Hamilton-Jacobi formulation. Journal of Computer Physics, 1988,79:12−49.

[2] Caselles V, Kimmel R, Sapiro G. Geodesic active contours. Int'l Journal on Computer Vision, 1997,22(1):61−97.

[3] Chan TF, Vese LA. Active contours without edges. IEEE Trans. on Image Processing, 2001,10(2): 266−277.

[4] Vese LA, Chan TF. A multiphase level set framework for image segmentation using the Mumford and Shah model. Int'l Journal of Computer Vision, 2002,50(3):271−293.

[5] Chen J, Tian J, Xue J, Dai YK. Level set method with multi-speed-function and its application in segmentation of medical images. Journal of Software, 2007,18(4):842−849 (in Chinese with English abstract). http://www.jos.org.cn/1000-9825/18/842.htm

[6] Mumford D, Shah J. Optimal approximations by piecewise smooth functions and associated variational problems. Communications on Pure and Applied Mathematics, 1989,42(4):577−685.

[7] Tsai A, Yezzi A, Willsky AS. Curve evolution implementation of the Mumford-Shah functional for image segmentation, denoising, interpolation, and magnification. IEEE Trans. on Image Processing, 2001,10(8):1169−1186.

[8] Tsai A, Yezzi A, Willsky AS. A curve evolution approach to smoothing and segmentation using the Mumford-Shah functional. In: Proc. of the IEEE Conf. Computer Vision Pattern Recognition. Hilton Head Island, 2000. 119−124.

[9] Gazit MH, Goldsher D, Kimmel R. Hierarchical segmentation of thin structures in volumetric medical images. In: Proc. of the 6th Int'l Conf. on Medical Image Computing and Computer-Assisted Intervention—MICCAI 2003. 2003. 562−569.

[10] Jeon M, Alexander M, Pedrycz W. Unsupervised hierarchical image segmentation with level set and additive operator splitting. Pattern Recognition Letter, 2005,26(10):1461−1469.

[11] Li S, Fevens T, Krzyzak A. A SVM-based framework for autonomous volumetric medical image segmentation using hierarchical and coupled level sets. In: Proc. of the Int'l Congress Series. 2004. 207−211.

[12] Li S, Fevens T, Krzyzak A. Semi-Automatic computer aided lesion detection in dental X-rays using variational level set. Pattern Recognition, 2007,40(10):2861−2873.

[13] Li S, Fevens T, Krzyzak A. An automatic variational level set segmentation framework for computer aided dental X-rays analysis in clinical environments. Computerized Medical Imaging and Graphics, 2006,30:65−74.

[14] Li S, Fevens T, Krzyzak A. Image segmentation adapted for clinical settings by combining pattern classification and level sets. In: Proc. of the7th Int’l Conf. on Medical Image Computing and Computer-Assisted Intervention—MICCAI 2004. 2004. 160−167.

[15] Perona P, Malik J. Scale-Space and edge detection using anisotropic diffusion. IEEE Trans. on Pattern Analysis and Machine Intelligence, 1990,12(7):629−639.

[16] Zhu FP, Tian J, Lin Y, Ge XF. Medical image segmentation based on level set method. Journal of Software, 2002,13(9):1866−1872 (in Chinese with English abstract). http://www.jos.org.cn/1000-9825/13/1866.htm

[17] Lu HY. Studies and applications of modeling techniques in active contours for medical image segmentation [Ph.D. Thesis]. Beijing: Peking University, 2006 (in Chinese with English abstract).

[18] Oshe S, Fedkiw R. Level Set Methods and Dynamic Implicit Surfaces. New York: Springer-Verlag, 2003. 23−93.

[19] Zhao HK, Chan T, Merriman B. A variational level set approach to multiphase motion. Journal of Computational Physics, 1996, 127(1):179−195.

[20] Rudin LI, Osher S, Fatemi E. Nonlinear total variation based noise removal algorithms. Physics D, 1992,60(1-4):259−268.

附中文参考文献:

[5] 陈健,田捷,薛健,戴亚康.多速度函数水平集算法及在医学分割中的应用.软件学报,2007,18(4),842−849. http://www.jos.org.cn/1000-9825/18/842.htm

[16] 朱付平,田捷,林瑶,葛行飞.基于 Level Set 方法的医学图像分割.软件学报,2002,13(9):1866−1872. http://www.jos.org.cn/1000-9825/13/1866.htm

[17] 吕红宇.医学图像分割中主动轮廓法的模型化研究及应用[博士学位论文].北京,北京大学,2006.

DUAN Chai-Jie was born in 1981. He is a Ph.D. candidate at Beijing Key Laboratory of Medical Physics and Engineering, Institute of Heavy Ion Physics, Peking University. His research areas are medical image segmentation and recognition.

MA Jing-Feng was born in 1974. He is a Ph.D. candidate at College of Computer Science, Zhejiang University. His research area is medical image processing.

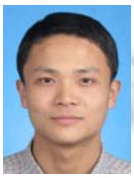

ZHANG Yi-Bao was born in 1985. He is a Ph.D. candidate at Beijing Key Laboratory of Medical Physics and Engineering, Institute of Heavy Ion Physics, Peking University. His research area is radiotherapy.

HOU Kai was born in 1982. He is a software engineer, graduated from the University of the South China, Nuclear Science and Technology Institute, and majored in Biomedical Engineering. Now he works at Beijing Healthware Science & Technology Inc.

BAO Shang-Lian was born in 1945. He is a professor and doctorial supervisor at Peking University, the director of Research Center for Tumor Diagnosis and Radio-therapeutical Physics and Beijing City Key Lab of Medical Physics and Engineering. His research areas are medical imaging physics, radiotherapy physics and medical image processing.